

Micro-computerized tomography analysis of alveolar bone loss in ligature- and nicotine-induced experimental periodontitis in rats

Y.-F. Liu¹, L.-A. Wu¹, J. Wang²,
L.-Y. Wen¹, X.-J. Wang¹

¹Department of Pediatric Dentistry, School of Stomatology, Fourth Military Medical University, Xi'an, Shaanxi, China and ²Department of Osteology, Xijing Hospital, Fourth Military Medical University, Xi'an, Shaanxi, China

Liu Y-F, Wu L-A, Wang J, Wen L-Y, Wang X-J. Micro-computerized tomography analysis of alveolar bone loss in ligature- and nicotine-induced experimental periodontitis in rats. *J Periodont Res* 2010; 45: 714–719. © 2010 John Wiley & Sons A/S

Background and Objective: Nicotine reportedly is a risk factor for periodontitis, but accurate data regarding nicotine-induced alveolar bone loss is lacking. The aim of this study was to quantitatively assess alveolar bone loss in ligature- and nicotine-induced periodontitis in rats using micro-computerized tomography (micro-CT).

Material and Methods: Thirty-six adult male rats were treated by placing silk ligatures around the cervixes of the right second maxillary molar; the contralateral tooth was untreated. After ligation, the animals were randomly divided into three groups: group A received intraperitoneal injections of saline solution, group B received 0.83 mg of nicotine/kg/d, and group C received 1.67 mg of nicotine/kg/d. Six animals in each group were killed on days 14 and 28 after ligature placement, and then micro-CT examinations were conducted.

Results: In all groups, bone mineral density (BMD), bone volume fraction (BVF), trabecular number (Tb.N) and trabecular thickness (Tb.Th) values of the ligated sides were significantly lower than those of the unligated sides ($p < 0.001$), whereas alveolar bone height loss (ABHL) and trabecular separation (Tb.Sp) of the ligated sides were significantly higher than those of the unligated sides ($p < 0.001$). Compared with the control group, nicotine administration increased the ABHL value and decreased the BMD, BVF and Tb.Th values of both sides in a dose-dependent manner ($p < 0.05$).

Conclusion: Our results confirmed that ligature could cause significant loss in the trabecula of alveolar bone, and daily administration of nicotine resulted in further bone loss and microstructure deterioration.

Xiao-jing Wang, Department of Pediatric Dentistry, School of Stomatology, Fourth Military Medical University, Xi'an, 710032, Shaanxi, China
Tel: +86 29 84776087
Fax: +86 29 84776083
e-mail: wxjing@fmmu.edu.cn

Key words: nicotine; Sprague–Dawley rats; periodontitis; X-ray microtomography; alveolar bone loss

Accepted for publication February 12, 2010

Periodontitis is a chronic inflammatory disease that results in periodontium destruction, pocket formation and

alveolar bone loss. Tobacco smoking reportedly is one of the risk factors for periodontitis (1–5). The relative risk

for smokers to develop destructive periodontitis has been estimated to be 5- to 20-fold greater than that of non-

smokers (1). However, the direct effects of smoking on periodontal tissues are still not well understood.

Tobacco smoke contains a complex mixture of substances. Nicotine, one of the toxic products in cigarette smoke, has been investigated for its possible role in the process of periodontal breakdown. *In vivo* studies using histologic techniques revealed that, compared with saline solution, daily administration of nicotine might enhance the effects of local factors that produce periodontal bone loss in the furcation region (6). In addition, dose-dependent bone loss in the molar furcation region was observed when a gradient of nicotine concentrations was applied (7,8), which indicated a close association between nicotine and periodontal morbidity.

Periodontitis is characterized by alveolar bone loss. Several methods can be used to measure alveolar bone loss in periodontitis, including morphometric, radiologic and histologic techniques (7–10). However, these methods provide only linear or two-dimensional (2D) information because they measure horizontal bone loss; they do not yield data about the three-dimensional (3D) intrabony changes that occur during periodontal infection.

Recent studies have shown that micro-computerized tomography (micro-CT) is more sensitive in measuring bone mass and bone microstructure than conventional methods (11–15). The micro-CT technique, which has been widely used to study bone metabolism in animals (15–17), is a novel way to evaluate 3D structures of hard tissues. High-resolution micro-CT analysis can be used to build a 3D bone model and to analyze the data in a highly precise and nondestructive way (17). The images reconstructed by micro-CT scanning provide 3D information about internal hard tissues. Thus, by measuring bone height, bone density, bone structure and other parameters using micro-CT, detailed information about bone changes over time can be obtained.

Although previous studies revealed that nicotine can facilitate periodontal bone loss, accurate data about the 3D

volumetric loss and microstructure deterioration of the alveolar bone are lacking. Therefore, in this study we quantitatively measured the effect of nicotine on alveolar bone loss and microstructure in a ligature-induced animal model of periodontitis using micro-CT.

Material and methods

Animals

Thirty-six male Sprague–Dawley rats (8–10 wk of age, 200–230 g; Laboratory Animal Center, the Fourth Military Medical University, Xi'an, China) were used in this study. At the start of the experiment, no clinical signs of gingival inflammation were observed among the animals. The animals were housed in individual wire cages in a temperature- and humidity-controlled room ($23 \pm 1^\circ\text{C}$ and $60 \pm 5\%$ relative humidity) with a 12-h light/dark cycle. All animals were allowed to acclimate to the laboratory environment for 1 wk before surgical procedures were carried out. All experimental animal use protocols were approved by the Animal Care Committee of School of Stomatology, the Fourth Military Medical University.

Experimental design

Animal experiments—Based on the literature, five rats per group at each time-point were needed (18). In our study we used more rats – 12 rats in each group (six rats for each time-point) – in case some died during the experimental period following the induction of periodontitis. Fortunately, none of the rats died before being killed.

Under anesthesia with sodium pentobarbital, 36 adult male Sprague–Dawley rats were treated as follows: silk ligatures (no. 3-0; Golden Circle Medical Limited Corporation, Shanghai, China) were tied around the cervixes of the right second maxillary molar, while the contralateral tooth was untreated (19). Subsequently, the animals were randomly divided into three groups (12 animals per group). Each group received daily intraperitoneal injections

of saline solution (group A), 0.83 mg of nicotine (Sigma, St Louis, MO, USA)/kg/d (group B), or 1.67 mg of nicotine/kg/d (group C). In the present study, the two doses of nicotine (0.83 and 1.67 mg/kg/d) used were representative of humans who smoke 10 and 20 cigarettes (containing 2.0 mg of nicotine each) per day (19). Six animals in each group were randomly selected and killed on days 14 and 28 after ligature placement. The maxillae were harvested and fixed in 10% formalin solution for 48 h. After fixation, alveolar bone was examined using a micro-CT scanner (eXplore Locus SP, GE Healthcare, Waukesha, WI, USA).

Micro-CT scan

Scanning method—The computed tomography parameters were as follows: (i) the image pixel size was set to 1024×1024 ; (ii) the slice thickness was set to $14 \mu\text{m}$; (iii) the image magnification was set to 10 \times ; (iv) the X-ray tube voltage was set to 50 kV; and (v) the anode electrical current was set to 0.1 mA. Three-dimensional images were reconstructed using the micro-reconstruct software (GE Healthcare, Waukesha, WI, USA).

Linear (2D) measurement—The micro-view explore analysis software (GE Healthcare) was used to visualize and quantify the image data on a personal computer. All scans were re-oriented before analysis to uniformly align the scan axes and anatomical position (i.e. proximal–distal, buccal–lingual and medial–lateral). Alveolar bone height loss (ABHL) measurements were taken (in mm) from the cemento–enamel junction (CEJ) to the alveolar bone crest along the distal and medial root of the second molars (both the ligated tooth and the unligated tooth) (Fig. 1). All images were re-oriented so that both the CEJ and the root apex appeared in the same micro-CT slice.

Volumetric (3D) measurement—Volumetric measurements followed the procedure proposed by Park *et al.* (17), with slight modification. As shown in Fig. 2, measurements were made following the selection of 3D regions of

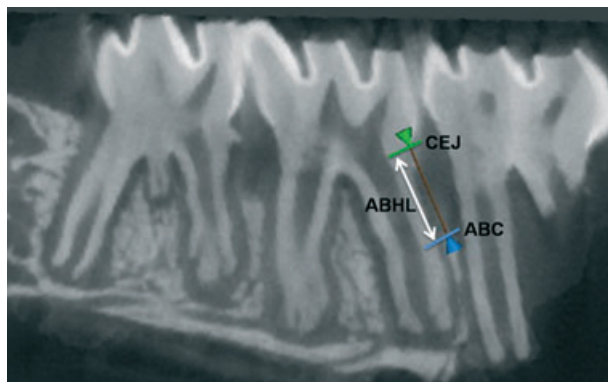


Fig. 1. Linear measurement of alveolar bone height loss (ABHL). The ABHL was assessed from images of two-dimensional (2D) micro-computerized tomography (micro-CT) sections. The distances (in mm) from the cemento–enamel junction (CEJ) to the alveolar bone crest (ABC) along the distal and medial root of the second molar were measured.

interest (ROI). Examiners were guided by morphological landmarks when drawing ROIs. In the case of periodontal defects resulting from experimental periodontitis, most bone loss was noted around the roots of the teeth, below the roofs of the furcations (ROFs) and above the root apex.

The most distal root of M1 (d-M1) and the most medial root of M3 (m-M3) served as end point landmark borders because they were the most consistent among specimens. Thus, the re-orientation of specimens from examiner to examiner relied on capturing these landmarks, which essentially maximized the ROI of the alveolar bone housing the alveolus (Fig. 2).

To maximize the quantification of bone, to minimize the inclusion of tooth roots and to use as many reproducible

landmarks as possible, we drew the desired region contours from the landmarks ROF to root apex at regular intervals (Fig. 2). All contours were drawn immediately below the ROFs in the coronal plane and then in the apical direction. Using an advanced ROI tool, 2D contours were drawn at regular intervals (every six data planes). Some of the contours were drawn at smaller intervals (one to two planes) to minimize the effects of root contour variability. Contours were drawn until the apices of d-M1 and m-M3 were reached. Next, a 3D ROI was generated using the micro-view image analysis software based on the resultant 2D contours. Finally, parameters in the volume of selected and contour-drawn ROIs were estimated (Table 1). Two experienced observers

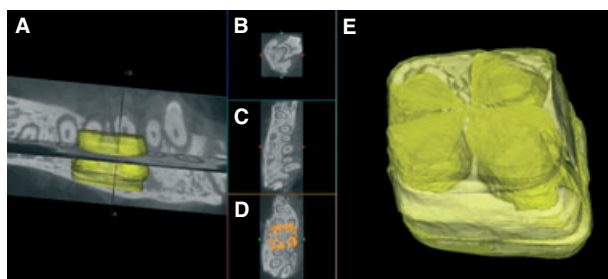


Fig. 2. Method for creating three-dimensional (3D) regions of interest (ROI) used in volumetric measurement of alveolar bone loss. (A) 3D ROI tools were selected. Border lines were drawn along the roots of the second molar using landmarks of the most distal root of M1 (d-M1) and the most medial root of M3 (m-M3) from the roof of the furcation to the root apex (B, proximal–distal; C, buccal–lingual; D, medial–lateral), then a 3D ROI was generated by the software based on the resultant two-dimensional (2D) contours. (E) Alveolar bone to be analyzed was constructed following the border of the 3D ROI.

who were blind to group assignment analyzed all images twice, and then mean values from the two observers were averaged.

Statistical analysis— All values were expressed as means \pm standard deviation. Statistical analyses were performed using SPSS 12.0 software (SPSS Inc, Chicago, IL, USA). Statistical significance was set at $p < 0.05$. Multiple comparisons were used to compare parameters of the tested samples between the different groups and time of observations. The paired Student's *t*-test was used to compare data between bilateral sides (left and right). Pearson's correlation was used to examine the correlation between doses of nicotine and each parameter.

Results

Three dimensional images from micro-CT scans revealed a clear decrease in the alveolar bone around the second molar in the ligated group compared with the unligated control group (Fig. 3).

Linear micro-CT measurements

Ligation significantly increased the ABHL of the right second maxillary molar compared with the contralateral molar ($p < 0.001$). Intergroup analysis revealed that, compared with the control group, nicotine administration enhanced the ABHL in a dose-dependent manner ($p < 0.05$). On day 28, the ABHL of group C was 0.61 ± 0.14 (left, unligated) and 1.39 ± 0.09 mm (right, ligated), which was significantly higher than that of group B (0.39 ± 0.10 , 1.31 ± 0.06 mm) ($p < 0.01$, $p < 0.05$), and the values for groups B and C were significantly higher than that of group A (0.30 ± 0.06 , 0.94 ± 0.07 mm) ($p < 0.01$, $p < 0.01$) (Fig. 4A).

Volumetric micro-CT measurements

Paired *t*-tests showed that in all groups, bone mineral density (BMD, Fig. 4B), bone volume fraction (BVF, Fig. 4C), trabecular thickness (Tb.Th, Fig. 4D) and trabecular number

Table 1. Parameters estimated by micro-computerized tomography (micro-CT) in this study

Parameters	Abbreviations	Definitions	Trends during osteoporosis
Bone mineral density	BMD	BMD was defined as the volumetric mineral density in the region of interest (ROI) and represented the apparent bone mineral density of trabecula	Decrease
Bone volume fraction	BVF	BVF was calculated from bone volume (BV) and total volume (TV) as BV/TV	Decrease
Bone trabecular thickness	Tb.Th	Tb.Th was calculated by applying the distance transformation by filling maximal spheres in the bone structures	Decrease
Trabecular separation	Tb.Sp	Tb.Sp was calculated by applying the distance transformation by filling maximal spheres in the nonbone structures	Increase
Trabecular number	Tb.N	Tb.N was taken as the inverse of the mean distance between the mid-axes of the observed structure under observation	Decrease

cant correlation between nicotine and bilateral BMD, BVF, Tb.Sp and Tb.Th ($p < 0.01$). By contrast, we did not find a significant correlation between nicotine and Tb.N parameters, as shown in the results of the intergroup analysis (Table 2).

Discussion

The present study introduced a 3D technique that enabled us to illustrate the state of the alveolar bone in the rat model of ligature- and nicotine-induced experimental periodontitis and to provide accurate data about the volumetric alveolar bone changes that occurred during the experiment. Using the 3D images reconstructed by the micro-view imaging system, absorption of bone was observed around the area of the silk thread ligation. The administration of nicotine further exacerbated this alveolar bone loss.

Smoking is associated with excessive destruction of the supporting periodontal tissues, resulting in pocket formation, bone loss and eventually tooth loss (1). The relative risk of developing destructive periodontitis can be about 5–20-fold higher in smokers compared with nonsmokers. Two-dimensional linear analysis showed that silk thread ligation resulted in significant alveolar bone absorption by day 14. The alveolar bone loss was more severe on day 28. Nicotine injection after ligation further increased the loss of alveolar bone on days 14 and 28. We also found that without ligation, nicotine itself caused alveolar bone loss in a dose-dependent manner, albeit its effects were relatively slight compared with the effects of ligation. The effects of nicotine on alveolar bone loss observed in our model were in agreement with clinical data that showed a dose-effect relationship between cigarette consumption and the probability of having advanced periodontal disease (3,4,20). The effects of smoking on periodontal tissues depend on the number of cigarettes smoked daily and the duration of the habit (2).

In osteoporosis, the values of BMD, BVF, Tb.N and Tb.Th decreased and that of Tb.Sp increased (21). The volumetric measurements taken from our

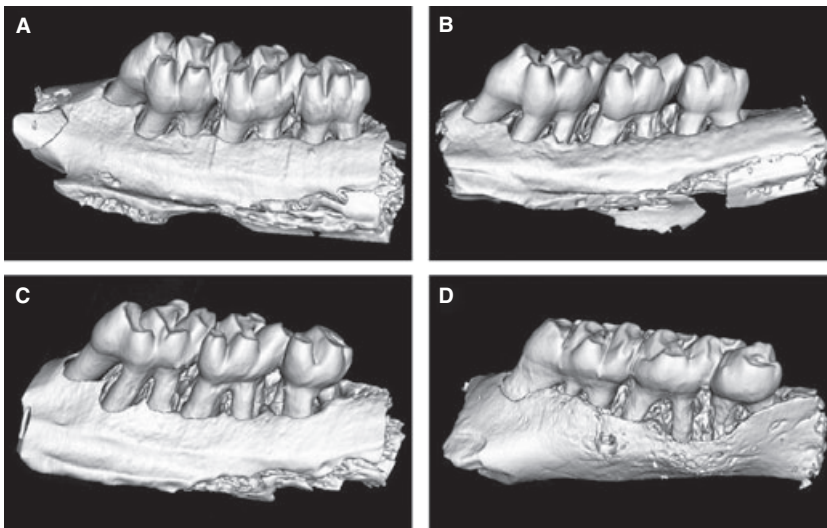


Fig. 3. Surface-reconstructed images of the alveolar bone on day 28. Representative images are shown from (A) the unligated side of saline group A, (B) the ligated side of group A, (C) the ligated side of group B (daily administration of 0.83 mg/kg of nicotine) and (D) the ligated side of group C (daily administration of 1.67 mg/kg of nicotine).

(Tb.N, Fig. 4E) values of the ligated side were significantly lower than those of the nonligated side ($p < 0.001$), whereas the trabecular separation (Tb.Sp, Fig. 4F) of the ligated side was significantly higher than that of the nonligated side ($p < 0.001$). Intergroup analysis revealed that compared

with the control group, nicotine administration decreased the BMD, BVF and Tb.Th values of both sides in a dose-dependent manner ($p < 0.05$). However, no statistically significant differences in the Tb.N parameters between groups were found. Pearson's correlation analysis revealed a signifi-

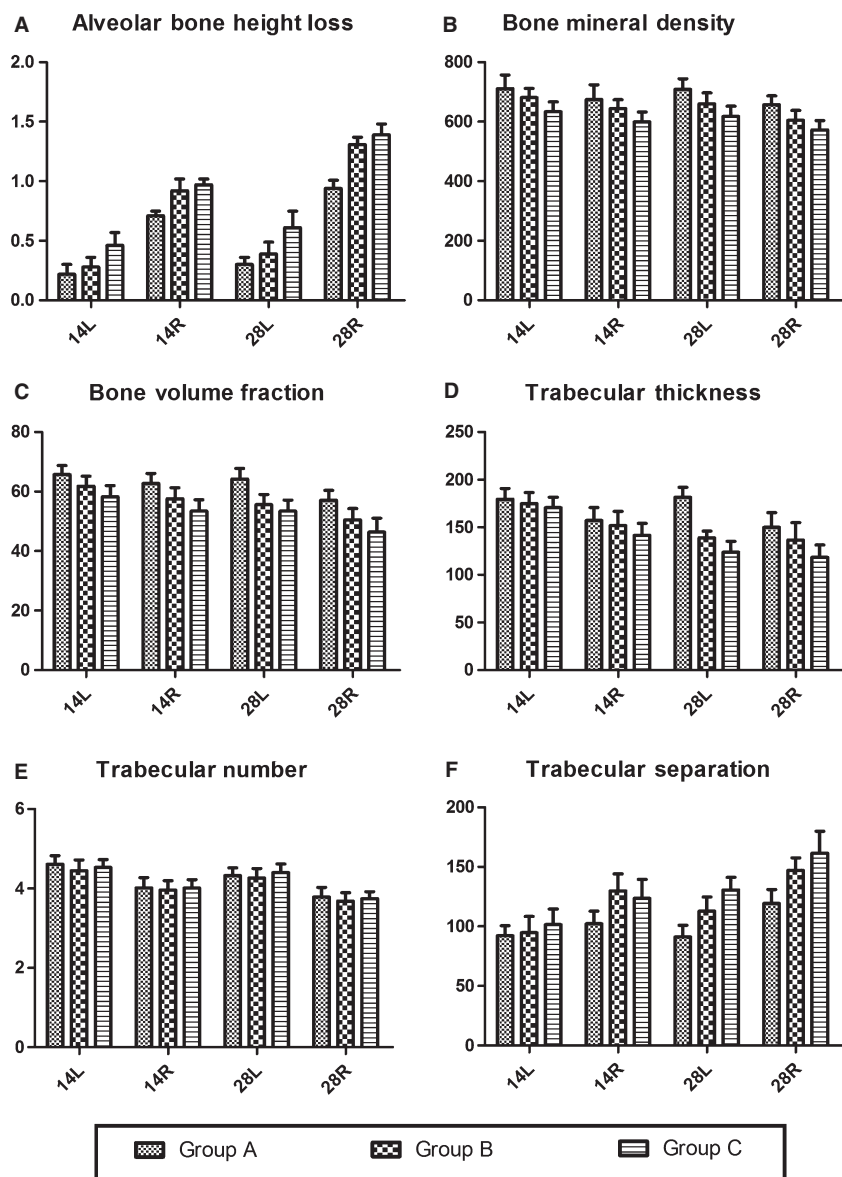


Fig. 4. Linear measurements of alveolar bone height loss and volumetric measurements of trabecular bone changes among group A (control), group B (daily administration of 0.83 mg/kg of nicotine) and group C (daily administration of 1.67 mg/kg of nicotine). (A) Alveolar bone height loss, (B) bone mineral density, (C) bone volume fraction, (D) trabecular thickness, (E) trabecular number, (F) trabecular separation. 14L, left/ unligated side on day 14; 14R, Right/ ligated side on day 14; 28L, left/ unligated side on day 28; 28R, Right/ ligated side on day 28.

Table 2. Linear correlation of parameters on day 28

Parameter	Tb.Th		Tb.N		Tb.Sp		BMD		BVF	
	Left	Right	Left	Right	Left	Right	Left	Right	Left	Right
N	18	18	18	18	18	18	18	18	18	18
Correlation	-0.866**	-0.730**	-0.141	-0.212	0.657**	0.623**	-0.725**	-0.709**	-0.710**	-0.781**
p-value	0.000	0.000	0.512	0.320	0.000	0.001	0.000	0.000	0.000	0.000

** $p < 0.001$.

BMD, bone mineral density; BVF, bone volume fraction; Tb.N, trabecular number; Tb.Sp, trabecular separation; Tb.Th, trabecular thickness.

3D alveolar bone model showed that in all groups the BMD, BVF, Tb.N and Tb.Th values of the ligated side were significantly lower than those of the nonligated side, whereas the Tb.Sp of the ligated side was significantly higher than that of the nonligated side. The increase in the dose of nicotine correlated well with decreased values of BMD, BVF, Tb.Sp and Tb.Th on both the ligated and nonligated sides, which clearly indicated an association between nicotine and periodontal bone microstructure deterioration. This finding illustrates that nicotine deteriorates the microstructure of trabecular bone, and this process is difficult to detect using conventional methods. The results of our experiment are consistent with a clinical study showing that smoking had a negative effect on alveolar bone, as assessed radiographically in a group of well-motivated young adults without periodontitis (22). Together these data demonstrate a close relationship among smoking, nicotine and periodontitis.

In conclusion, the present study described the 3D quantification of alveolar bone loss during the process of periodontitis in rats. Our results confirmed that ligature could cause significant changes in the trabecula of alveolar bone, and daily administration of nicotine resulted in further bone loss and microstructure deterioration in a dose-dependent manner.

Acknowledgements

This work was supported by grants from the National Natural Science Foundation of China (NSFC grants 30572045 and 30973315). The authors are grateful to Dr Sumin Guan for her critical reading of the manuscript.

References

- Bergstrom J. Tobacco smoking and chronic destructive periodontal disease. *Odontology* 2004;**92**:1–8.
- Calsina G, Ramon JM, Echeverria JJ. Effects of smoking on periodontal tissues. *J Clin Periodontol* 2002;**29**:771–776.
- Ojima M, Hanioka T, Tanaka K, Inoshita E, Aoyama H. Relationship between smoking status and periodontal conditions: findings from national databases in Japan. *J Periodontol Res* 2006;**41**:573–579.
- Do LG, Slade GD, Roberts-Thomson KF, Sanders AE. Smoking-attributable periodontal disease in the Australian adult population. *J Clin Periodontol* 2008;**35**:398–404.
- Kibayashi M, Tanaka M, Nishida N *et al*. Longitudinal study of the association between smoking as a periodontitis risk and salivary biomarkers related to periodontitis. *J Periodontol* 2007;**78**:859–867.
- Nociti FH Jr, Nogueira-Filho GR, Primo MT *et al*. The influence of nicotine on the bone loss rate in ligature-induced periodontitis. A histometric study in rats. *J Periodontol* 2000;**71**:1460–1464.
- Nociti FH Jr, Nogueira-Filho GR, Tramontina VA *et al*. Histometric evaluation of the effect of nicotine administration on periodontal breakdown: an in vivo study. *J Periodontol Res* 2001;**36**:361–366.
- Bosco AF, Bonfante S, de Almeida JM, Luize DS, Nagata MJ, Garcia VG. A histologic and histometric assessment of the influence of nicotine on alveolar bone loss in rats. *J Periodontol* 2007;**78**:527–532.
- Benatti BB, Cesar-Neto JB, Goncalves PF, Sallum EA, Nociti FH Jr. Smoking affects the self-healing capacity of periodontal tissues. A histological study in the rat. *Eur J Oral Sci* 2005;**113**:400–403.
- Hausmann E. Radiographic and digital imaging in periodontal practice. *J Periodontol* 2000;**71**:497–503.
- Boyd SK, Davison P, Muller R, Gasser JA. Monitoring individual morphological changes over time in ovariectomized rats by in vivo micro-computed tomography. *Bone* 2006;**39**:854–862.
- Balto K, Muller R, Carrington DC, Dobeck J, Stashenko P. Quantification of periapical bone destruction in mice by micro-computed tomography. *J Dent Res* 2000;**79**:35–40.
- Barou O, Valentin D, Vico L *et al*. High-resolution three-dimensional micro-computed tomography detects bone loss and changes in trabecular architecture early: comparison with DEXA and bone histomorphometry in a rat model of disuse osteoporosis. *Invest Radiol* 2002;**37**:40–46.
- Cortet B, Chappard D, Boutry N, Dubois P, Cotten A, Marchandise X. Relationship between computed tomographic image analysis and histomorphometry for micro-architectural characterization of human calcaneus. *Calcif Tissue Int* 2004;**75**:23–31.
- Gielkens PF, Schortinghuis J, de Jong JR *et al*. A comparison of micro-CT, micro-radiography and histomorphometry in bone research. *Arch Oral Biol* 2008;**53**:558–566.
- Schouten C, Meijer GJ, van den Beucken JJ, Spauwen PH, Jansen JA. The quantitative assessment of peri-implant bone responses using histomorphometry and micro-computed tomography. *Biomaterials* 2009;**30**:4539–4549.
- Park CH, Abramson ZR, Taba M Jr *et al*. Three-dimensional micro-computed tomographic imaging of alveolar bone in experimental bone loss or repair. *J Periodontol* 2007;**78**:273–281.
- Scheibe PO. Number of samples — hypothesis testing. *Nucl Med Biol* 2008;**35**:3–9.
- Azoubel MC, Menezes AM, Bezerra D, Oria RB, Ribeiro RA, Brito GA. Comparison of etoricoxib and indomethacin for the treatment of experimental periodontitis in rats. *Braz J Med Biol Res* 2007;**40**:117–125.
- Meisel P, Schwahn C, Gesch D, Bernhardt O, John U, Kocher T. Dose-effect relation of smoking and the interleukin-1 gene polymorphism in periodontal disease. *J Periodontol* 2004;**75**:236–242.
- Lespessailles E, Chappard C, Bonnet N, Benhamou CL. Imaging techniques for evaluating bone microarchitecture. *Joint Bone Spine* 2006;**73**:254–261.
- Rosa GM, Lucas GQ, Lucas ON. Cigarette smoking and alveolar bone in young adults: a study using digitized radiographs. *J Periodontol* 2008;**79**:232–244.

This document is a scanned copy of a printed document. No warranty is given about the accuracy of the copy. Users should refer to the original published version of the material.